Research in Astron. Astrophys. **2013** Vol. **13** No. **9**, 1097–1106
http://www.raa-journal.org *http://www.iop.org/journals/raa*

***R**esearch in*
***A**stronomy and*
***A**strophysics*

Diffuse emission of TeV neutrinos and gamma-rays from young pulsars by photomeson interaction in the Galaxy

Zhi-Xiong Li[1], Gui-Fang Lin[2,3] and Wei-Wei Na[4]

[1] Department of Physics, Yunnan University, Kunming 650091, China; *zhixiongli456789@gmail.com*
[2] Yunnan Astronomical Observatory, National Astronomical Observatories, Chinese Academy of Sciences, Kunming 650011, China
[3] Laboratory for the Structure and Evolution of Celestial Objects, Chinese Academy of Sciences, Kunming 650011, China
[4] Department of Physics, Yuxi Normal University, Yuxi 653100, China; *naww@yxnu.net*

Received 2013 January 25; accepted 2013 April 11

Abstract It is generally believed that young, rapidly rotating pulsars are important sites of particle acceleration, in which protons can be accelerated to relativistic energy above the polar cap region if the magnetic moment is antiparallel to the spin axis ($\boldsymbol{\mu} \cdot \boldsymbol{\Omega} < 0$). To obtain diffuse neutrinos and gamma-rays at TeV that originate in our Galaxy, we use the Monte Carlo method to generate a sample of young pulsars with ages less than 10^6 yr in our galaxy; the neutrinos and high-energy gamma-rays can be produced through a photomeson process with the interaction of energetic protons and soft X-ray photons ($p + \gamma \rightarrow \Delta^+ \rightarrow n + \pi^+ / p + \pi^0$) for a single pulsar, and these X-ray photons come from the surface of the neutron star. The results suggest that the flux of diffuse neutrinos at TeV energies is lower than the background flux, indicating they are difficult to detect using current neutrino telescopes.

Key words: pulsars: general — stars: neutron — neutrinos and gamma-rays: stars — elementary: neutrinos

1 INTRODUCTION

Very high-energy ($E > 100$ GeV) neutrinos and gamma-rays from astrophysical objects can provide a clear indication about the origins of Galactic and extragalactic cosmic rays. The radiation probably comes from gamma-ray bursts (GRBs), active galactic nuclei (AGNs), pulsars, etc. In our Galaxy, most high-energy gamma-rays and neutrinos are associated with pulsars, supernova remnants and pulsar nebulae (Bednarek et al. 2005; Kistler & Beacom 2006). Young pulsars are persistent and periodic sources; their radiation also travels shorter distances to Earth than does that from extragalactic sources. If they emit high-energy neutrinos/gamma-rays, we can spend a longer time searching for the signals. If the TeV neutrinos and gamma-rays can be detected from pulsars, it will help improve our knowledge about the hadronic process taking place in the magnetosphere.

Recently, studies (Link & Burgio 2005, 2006; Bhadra & Dey 2009; Jiang et al. 2007) have shown that if the magnetic moment of a pulsar (with age less than 10^6 yr) is antiparallel to its spin axis

($\boldsymbol{\mu} \cdot \boldsymbol{\Omega} < 0$), Δ-resonance will be produced when ions accelerated by the pulsar interact with these thermal radiation fields. These high-energy neutrinos and gamma-rays then decay by Δ-resonance. Link & Burgio (2006) (hereafter LB) considered the situation where, near the surface of the neutron stars, protons or heavier ions can be accelerated by polar caps to PeV energy. When the thermal radiation field of a pulsar interacts with accelerated ions having PeV energy, the Δ-resonance state may occur. This process is effective, and pions subsequently decay to muon neutrinos or gamma-rays. LB calculated the energy spectrum of muon neutrinos from some pulsars and estimated the event rates on Earth. The spectrum sharply rises at $\sim$50 TeV, corresponding to the onset of the resonance. The flux drops with neutrino energy as ϵ_ν^{-2} up to an upper energy cut-off that is determined by either kinematics or the maximum energy to which protons are accelerated. Bhadra & Dey (2009) estimated the TeV gamma-ray flux on the Earth from a few young, nearby pulsars and compared it with observations; they found that proper consideration of the effect of the polar cap geometry in flux calculation is important, and subsequently revised the event rates.

In this paper we find the ratio of polar cap area to neutron star surface area, denoted as η, is double that given by Bhadra & Dey (2009). We use revised polar cap geometry to calculate the flux of TeV neutrinos and the gamma-ray spectrum from some young pulsars, and estimate the event rates on Earth. In order to estimate the flux of diffuse TeV neutrinos and gamma-rays from the Galactic plane, a sample of pulsars in our galaxy is required. We simulate the pulsar sample with a Monte Carlo (MC) method (Cheng & Zhang 1998; Zhang & Harding 2000; Jiang et al. 2007) and obtain the flux of diffuse neutrinos and gamma-rays at TeV energies from young pulsars in our galaxy.

In Section 2, we review the model of LB. In Section 3, we calculate the neutrino and gamma-ray spectrum from a single pulsar by a revised polar cap geometry. In Sections 4 and 5, we obtain a sample of young pulsars in our galaxy using the MC method, then estimate the emission of diffuse neutrino and gamma-rays from these Galactic young pulsars. Lastly, the discussion and conclusions are presented.

2 THE MODEL OF NEUTRINOS AND GAMMA-RAYS FROM YOUNG PULSARS

Neutron stars have enormous magnetic fields ($B \geq 10^{12}$ G) and high rotation rates (tens of Hertz) which act as very powerful generators. Charges will be stripped off the highly conductive surface and accelerated somewhere above the stellar surface. The mechanisms of particle acceleration from pulsars have generally been divided into the polar gap model (Ruderman & Sutherland 1975; Arons & Scharlemann 1979; Daugherty & Harding 1996; Gonthier et al. 2002) and outer-gap model (Zhang et al. 2004; Cheng et al. 1986). In the former, particles are accelerated in a charge-depleted region near the magnetic pole of the neutron star. In the outer-gap, it will take place in the vacuum gaps between the neutral line and the last open line in the magnetosphere. Therefore, the region where acceleration occurs in the polar-gap model is close to the surface of the neutron star, whereas in the outer-gap model it is near the light cylinder.

In the polar gap model, because of large rotation-induced electric fields, particles can be extracted from the surface of the polar cap, then be accelerated, and finally form the primary beam. The potential drop across the field of a pulsar from the magnetic pole to the last field line open to infinity is $\Delta\phi = B_{\rm s}R^3\Omega^2/2c^2$ (Goldreich & Julian 1969), where $B_{\rm s}$ is the strength of the dipole component of the field at the magnetic poles ($B_{\rm s} \sim 10^{12}$ G), $R = 10^6 R_6$ is the radius of the neutron star, $p_{\rm m}$ is the spin period in milliseconds, $\Omega = 2\pi/p$ is the angular velocity (where p is the period) and c is the speed of light. The magnitude of the potential drop $\Delta\phi$ could be as high as $7 \times 10^{18} B_{12} P_{\rm ms}^{-2}$ V ($B_{\rm s} \equiv B_{12} \times 10^{12}$) (Goldreich & Julian 1969). LB consider that if the electric field has no or little screening and $\boldsymbol{\mu} \cdot \boldsymbol{\Omega} < 0$ (expected to hold for half of all pulsars), ions and protons will be accelerated to PeV energy near their surface. $\boldsymbol{\mu}$ is the magnetic moment, and $\boldsymbol{\Omega}$ is angular velocity. Protons or ions accelerated by pulsars will interact with thermal radiation they produce. If the accelerated particles have sufficient energy and exceed the threshold energy for the

Δ-resonance state (Δ^+ is an excited state of a proton, with a mass of 1232 MeV), the Δ-resonance state may occur. The threshold condition for the production of a Δ-resonance state in the $p-\gamma$ interaction is given by

$$\epsilon_p \epsilon_\gamma (1-\cos\theta_{p\gamma}) \geq 0.3\ \mathrm{GeV}^2\,, \tag{1}$$

where ϵ_p and ϵ_γ are the proton and photon energy respectively, and $\theta_{p\gamma}$ is the incidence angle between the proton and the photon in the lab frame. Young pulsars typically have temperatures of $T_\infty \simeq 0.1$ keV, and photon energy $\epsilon_\gamma = 2.8kT_\infty(1+z_{\rm g}) \sim 0.4$ keV, where $z_{\rm g}\approx 0.4$ is the gravitational redshift and T_∞ is the surface temperature measured at infinity. In a young pulsar's atmosphere, the condition for producing Δ-resonance is $B_{12}P_{\rm ms}^{-2}T_{0.1{\rm keV}} \geq 3\times10^{-4}$ (Link & Burgio 2005; Link & Burgio 2006), where $T_{0.1{\rm keV}} \equiv (kT_\infty/0.1\ {\rm keV})$ and $T_\infty \sim 0.1$ keV is the typical surface temperature of young pulsars. This condition holds for many young pulsars, so Δ-resonance could exist in the atmosphere of many pulsars. Gamma-rays and neutrinos subsequently decay through the following channels

$$p+\gamma \rightarrow \Delta^+ \rightarrow \begin{cases} p+\pi^0 \rightarrow p+2\gamma, \\ n\pi^+ \rightarrow n+{\rm e}^+ +\nu_e+\nu_\mu+\bar{\nu_\mu}. \end{cases}$$

Based on the LB model, we estimate the flux of neutrinos and gamma-rays emmited from pulsars. The flux of protons accelerated by the polar gap can be estimated as

$$I_{\rm pc} = cf_{\rm d}(1-f_{\rm d})n_0 A_{\rm pc}\,, \tag{2}$$

where $n_0(r) \equiv B_{\rm s}R^3\Omega/(4\pi Ze\,c\,r^3)$ is the Goldreich-Julian density of ions at distance r, and $f_{\rm d}<1$ is the fraction of the space charge that is depleted in the region where acceleration occurs. It is a model-dependent quantity ($f_{\rm d}=0$ corresponds to no depletion and $f_{\rm d}=1$ is full depletion), so the density in the depleted gap can be written as $f_{\rm d}(1-f_{\rm d})n_0$, where $A_{\rm pc}=\eta 2\pi R^2$ is the area of the polar cap, and η is the ratio of polar cap area to half of the neutron star's surface area. When $\eta=1$, the polar cap area is half of the neutron star's surface area. LB (2006) and Jiang et al. (2007) calculate it using the surface area of a hemisphere. The typical radius $r_{\rm pc}=R(\Omega R/c)^{1/2}$ (Beskin et al. 1993), and the polar gap surface is $A_{\rm pc}=\pi r_{\rm pc}^2=\pi\Omega R^3/c$, so $\eta=\Omega R/(2c)$. It is possible that $\eta=\Omega R/(2c)$ is more appropriate. For young pulsars with surface temperature T_∞, the photon density close to the surface of the neutron star is $n_\gamma(R)=(a/2.8k)[(1+z_{\rm g})T_\infty]$, where a is the Stefan-Boltzman constant. Numerically $n_\gamma(R)\simeq 9\times10^{19}T_{0.1{\rm keV}}^3$. At radial distance r, photon density will be $n_\gamma(r)=n_\gamma(R)(R/r)^2$. The probability that a PeV energy proton starting from the pulsar surface will produce a Δ particle by interacting with the thermal field is given by $p_c=1-\int_R^r p(r)$ (Link & Burgio 2005), where $dP/P=-n_\gamma(r)\sigma_{p\gamma}dr$. Thus the total flux of gamma rays/neutrinos generated in pulsars from the Δ^+ resonance is

$$I = 2c\xi A_{\rm pc} f_{\rm d}(1-f_{\rm d})n_0 P_c\,, \tag{3}$$

where ξ is $4/3$ and $2/3$ for gamma-rays and muon neutrinos, respectively. At the distance d, the phase averaged gamma-ray/neutrino flux on Earth from a pulsar is

$$\phi \simeq 2c\xi\zeta\eta f_b f_{\rm d}(1-f_{\rm d})n_0\left(\frac{R}{d}\right)^2 P_c\,, \tag{4}$$

where f_b is the duty cycle of a neutrino or gamma-ray beam, ζ is the effect due to neutrino oscillation (the decays of pions and their muon daughters result in initial flavor ratios $\phi_{\nu_e}:\phi_{\nu_\mu}:\phi_{\nu_\tau}$ of nearly $1:2:0$, but at large distances from the source, the flavor ratio is expected to become $1:1:1$ due to maximal mixing of ν_μ and ν_τ). $\zeta=1$ and 1/2 are for gamma-rays and muon neutrinos respectively. We want to obtain the spectrum of neutrinos and gamma-rays using the following differential form

$$\frac{d\phi_\nu}{d\epsilon_\nu} = 2c\xi\zeta\eta f_b f_{\rm d}(1-f_{\rm d})n_0\left(\frac{R}{d}\right)^2\frac{dP_c}{d\epsilon_\nu}\,. \tag{5}$$

Taking $f_{\rm d} = 1/2$ and $Z = A = 1$ for estimating upper limits on the flux, the neutrino and gamma-ray energy flux is estimated as

$$\frac{d\phi_\nu}{d\epsilon_\nu} = 3 \times 10^{-8} \xi\zeta\eta f_b B_{12} p_{\rm ms}^{-1} d_{\rm kpc}^{-2} T_{0.1{\rm keV}} \frac{dP_c}{dx}\,, \tag{6}$$

where $d_{\rm kpc}$ is the distance of the pulsar from Earth, and dP_c/dx is the probability of a proton converting to a Δ^+ particle per unit energy interval. The details have been shown in equation (26) in LB.

3 TEV NEUTRINOS AND THE GAMMA-RAY SPECTRUM

We use Equation (6) to estimate the flux of neutrinos and gamma-rays, and take $Z = 1$ and $f_{\rm d} = 1/2$ throughout this work. We consider linear $(\gamma = 1)$ and quadratic $(\gamma = 2)$ proton acceleration laws. Linear acceleration corresponds to an accelerating field which is constant in space and quadratic acceleration grows linearly with height above the star. We calculate the flux of neutrinos and gamma-rays for the Crab pulsar, Vela pulsar, PSR B1509–58 and PSR B1706–44 when $\eta = \Omega R/2c$ as shown in Figures 1 and 2. The parameters describing the source are presented in Table 1.

Table 1 Parameters of Some Pulsars

Source	d (kpc)	p (ms)	B_{12} (G)	$T_{0.1{\rm keV}}$	f_b	$\frac{dN}{dAdt}$ (LB06) ($\rm km^{-2}\ yr^{-1}$)	$\frac{dN}{dAdt}$ ($\rm km^{-2}\ yr^{-1}$)
Crab	2	33	3.8	~ 1.7	0.14	45	0.151
Vela	0.29	89	3.4	0.6	0.04	25	0.0313
B1706 − 44	1.8	102	3.1	1	0.13	1	0.0038
B1509 − 58	4.4	151	0.26	1	0.26	5	0.0057

For both acceleration laws, the spectrum turns sharply at $\varepsilon_\nu \simeq 70^{-1}_{0.1{\rm keV}}$ TeV corresponding to the onset of Δ-resonance. At the highest energy it drops approximately as ϵ_ν^{-2}, because the conversion becomes restricted. The flux is lower by about three orders of magnitude when we use the pulsar surface for calculations. This is more consistent with the observed upper limits of gamma-ray fluxes. Numerical values of integrated gamma-ray fluxes at TeV energies are obtained for pulsars and listed in Table 2.

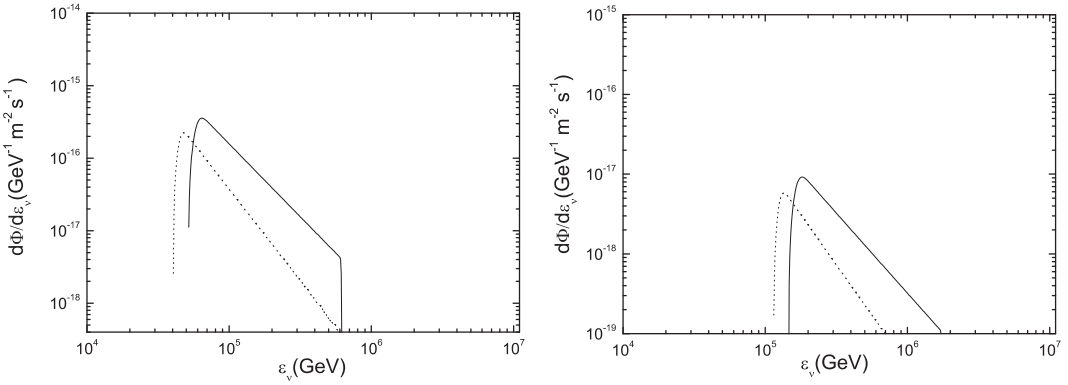

Fig. 1 The neutrino flux displayed for the Crab (*left panel*) and Vela (*right panel*) pulsars for the case of linear (*solid line*) and quadratic (*dotted line*) proton acceleration .

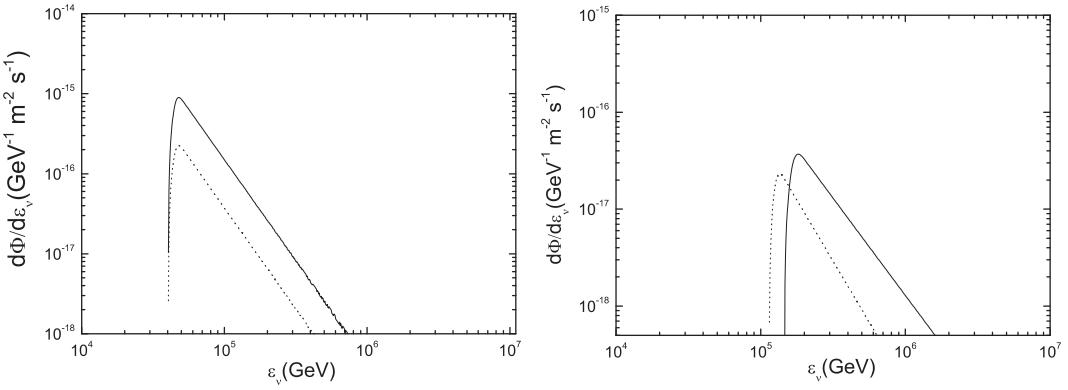

Fig. 2 The gamma-ray flux displayed for the Crab (*left panel*) and Vela (*right panel*) pulsars, for cases of linear (*solid line*) and quadratic (*dotted line*) proton acceleration.

Table 2 The integrated gamma-ray flux at TeV energies. This shows a comparison between the predicted and the observed values.

Source	$\eta = 1$ $(10^{-15}\ \mathrm{cm}^{-2}\ \mathrm{s}^{-1})$	$\eta = \Omega R/(2c)$ $(10^{-15}\ \mathrm{cm}^{-2}\ \mathrm{s}^{-1})$	Observed upper limit of integral flux $(10^{-15}\ \mathrm{cm}^{-2}\ \mathrm{s}^{-1})$
Crab	1038	3.297	8(56)
Vela	204.98	0.242	10(20)
$\mathrm{B1706-44}$	67.4773	0.0692	10(20)
$\mathrm{B1509-58}$	69.675	0.0484	10(20)

Notes: The observed upper limits for the Crab pulsar are due to Aharonian et al. (2006), whereas for the rest of the pulars the observed upper limits are due to Aharonian et al. (2007).

In Table 2, the gamma-ray flux estimated with $\eta = 1$ is obviously higher than the observed upper limits. However, with $\eta = \Omega R/2c$ it is a little lower and more consistent with the observed upper limits; thus taking $\eta = \Omega R/(2c)$ is more reasonable.

Large-area neutrino detectors use the Earth or ice as a medium for conversion of a muon neutrino to a muon. By detecting the Cherenkov light produced by neutrino interactions with high-energy muons below a detector on Earth, we can use the flux of neutrinos to estimate the count rate in the detector. The conversion probability in Earth is (Gaisser et al. 1995)

$$P_{\nu_\mu \to \mu} = 1.3 \times 10^{-6} (\epsilon_\nu / 1\ \mathrm{TeV})\,. \tag{7}$$

The muon event rate is

$$\frac{dN}{dAdt} = \int d\epsilon_\nu \frac{d\phi_\nu}{d\epsilon_\nu} P_{\nu_\mu \to \mu}\,. \tag{8}$$

In Table 1, the estimated count rates are presented in the last column for the Crab pulsar, Vela pulsar, PSR B1509–58 and PSR B1706–44, with $L = 0.1$ and linear acceleration. Expected count rates (LB) are shown in the penultimate column. Compared with the expected count rates shown in the last column, the expected count rates (LB) are higher, which means those cases that are detectable by IceCube will not present a strong signal (Abbasi et al. 2012). This result shows that IceCube data severely constrain the optimistic predictions of LB and Bhadra & Dey (2009), i.e. pulsars are unlikely to be a strong source of TeV neutrinos. Hence, proper consideration of the effect of a pulsar's polar cap geometry in flux calculations is important.

4 THE DIFFUSE NEUTRINOS AND GAMMA-RAY EMISSION FROM YOUNG GALACTIC PULSARS

Over 1800 radio pulsars are known (Manchester et al. 2005), and the ages of more than 400 pulsars are less than 10^6 yr, most of which are candidate sources. If the magnetic moment is antiparallel to the axis of rotation ($\mu \cdot \Omega < 0$), ions can be accelerated in the charge-depleted gap near the pulsar's surface, so young pulsars are also potential neutrino sources. Although some of them are likely to be weak sources, the total contribution could be significant. Therefore we use the MC method to simulate a pulsar sample with ages less than 10^6 yr, then determine which of them are neutrino pulsars in the sample. We also estimate the diffuse neutrino flux and gamma-ray flux. In other words, we will cumulate all the neutrino and gamma-ray flux with all potential pulsars in the sample.

4.1 Pulsar Sample Simulated by the Monte Carlo Method

We produce the population of young Galactic pulsars by the following assumptions (e.g. Sturner & Dermer 1996; Cheng & Zhang 1998; Zhang & Harding 2000; Zhang et al. 2004; Jiang & Zhang 2006). The pulsar sample is simulated with the MC method which is described by following steps (see Jiang et al. 2007 for details).

We use the conventional assumption for the birth rate of Galactic pulsars ($\sim 2/100\,\mathrm{yr}$) and enlarge it by 10 times, generating about 160 000 pulsars in the galactic plane during the past million years. In this sample about 3890 pulsars could be detected with radio. Many pulsars are not be observed because of the selection effect. Compared with the Australia Telescope National Facility (ATNF) pulsar catalog, our simulated sample is consistent with the distribution of observations. Normalized histograms showing the distribution of pulsar period, pulsar surface magnetic field and distance are shown in Figure 3. The shadowed histogram represents the ATNF sample, and the solid histogram represents the simulated sample. We also compare the distribution of galactic longitude and galactic latitude with the observed sample, which is shown in Figure 4. The shadowed histogram represents the ATNF sample and the solid histogram represents the simulated sample. Obviously, most pulsars are distributed in the region of galactic latitude $|b| < 5^\circ$, which demonstrates that our simulation successfully models this attribute.

4.2 The Diffuse Emission of Neutrinos and Gamma-rays from Young Pulsars

Diffuse neutrino and gamma-ray emissions, both from Galactic and extragalactic sources, are very interesting for astrophysics, particle physics and cosmology. The diffuse Galactic emission is produced by interactions with cosmic rays, mainly protons or electrons interacting with interstellar gas (via π^0-production and bremsstrahlung) and a radiation field (via inverse Compton scattering). We estimate the flux of gamma-rays and neutrinos $(d\phi_{v,i})/d\epsilon_\nu$ by using Equation (6). Then we can obtain the flux of neutrinos and gamma-rays from all pulsars

$$\phi(\epsilon_\nu) = \sum_{i=1}^{N} \frac{d\phi_{v,i}}{d\epsilon_\nu d\Omega_i}\,, \tag{9}$$

where N is the number of pulsars emitting gamma-rays or neutrinos, and $d\Omega_i$ is the solid angle for the ith pulsar; $d\Omega_i = 4\pi f_{b,i} \sim 1$. The results of neutrino energy flux are shown in Figure 5.

The energy flux sharply increases at about 50 TeV, corresponding to the onset of resonance. Most energy is emitted between 50 TeV and 0.8 TeV. After the onset of the resonance, the spectrum drops approximately as ϵ_ν^{-2}, because the phase space for conversion becomes restricted. Just like in the spectrum of a single pulsar, this behavior is typical for first-order Fermi acceleration (Abbasi et al. 2012). The linear acceleration of protons is about five times higher than the quadratic acceleration, so the linear acceleration is dominant.

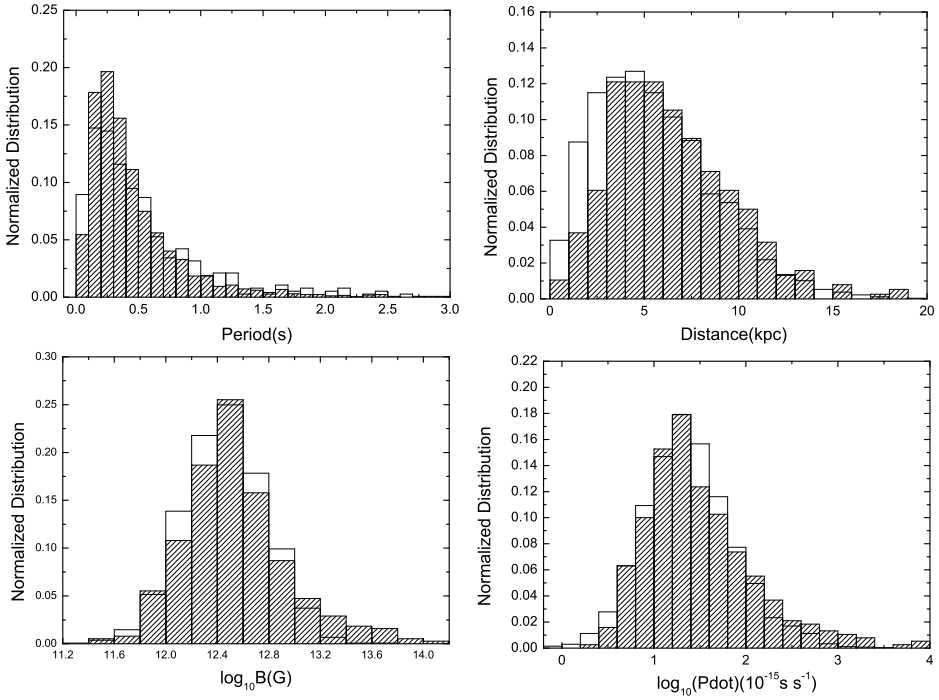

Fig. 3 Histogram showing the normalized distribution of pulsar period, distance, surface magnetic field and period. The shadowed histogram represents the observed sample. The solid histogram represents the simulated sample.

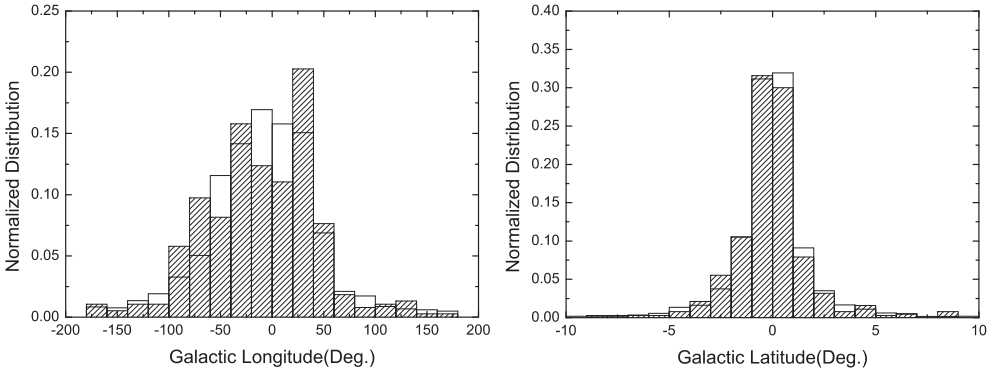

Fig. 4 Normalized histogram distribution of pulsars in Galactic longitude and Galactic latitude. The shadowed histogram represents the observed sample. The solid histogram represents the simulated sample.

From Figure 5, we can conclude that it will be more difficult to search for the signals of neutrinos, because these signals only slightly exceed the lower limit of background atmospheric neutrino flux. For comparison, we also give the predicted fluxes with sensitivities of detectors in AMANDA-II, ANTARES and IceCube. The AMANDA detector reached a sensitivity of

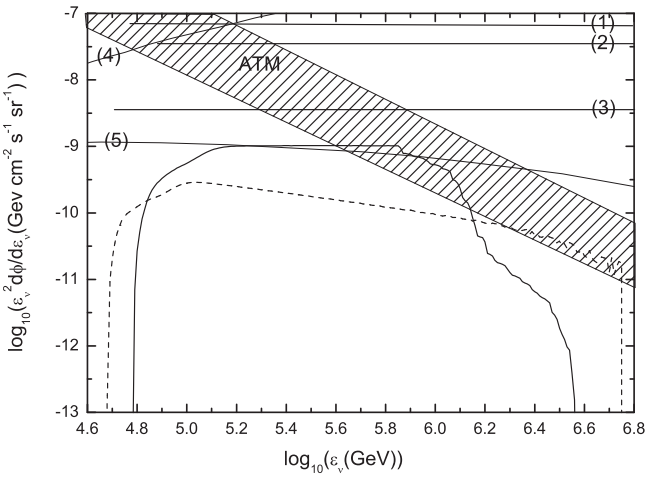

Fig. 5 The estimated diffuse neutrino flux from young pulsars in our Galaxy. The solid and dashed lines correspond to the fluxes computed for the cases of linear and quadratic proton acceleration respectively. The solid lines labeled (1), (2) and (3) represent the sensitivities of detectors in AMANDA-II, ANTARES and IceCube, respectively. The lines labeled (4) and (5) represent the predicted fluxes from AGNs (Stecker 2005) and GRBs (Liu & Wang 2013) respectively. The shadowed region is the background atmospheric neutrino flux (ATM) (Ribordy 2006).

8.9×10^{-8} GeV cm^{-2} s^{-1} sr^{-1} after the first four years of operat1ion in 2000–2003 (Hill et al. 2006). The sensitivity of the ANTARES detector reached $7.8 \pm 0.99 \times 10^{-8}$ GeV cm^{-2} s^{-1} sr^{-1} after one year of data on diffuse flux, and $3.9 \pm 0.7 \times 10^{-8}$ GeV cm^{-2} s^{-1} sr^{-1} after three years of data on diffuse flux (Montaruli 2005). The IceCube detectors have reached a sensitivity of $(2-7) \times 10^{-9}$ GeV cm^{-2} s^{-1} sr^{-1} after three years of operation (Ribordy 2006). It is clear that it is more difficult to detect the signals of neutrino flux from young pulsars, because the neutrino flux energy is lower than the background atmospheric neutrino flux. From Figure 5, we also compare the predicted diffuse neutrino fluxes from AGNs (Stecker 2005) and GRBs (Liu & Wang 2013). However, we can find that the diffuse neutrino fluxes from AGNs are larger than than those of young pulsars and GRBs at energies from 60 TeV to 3 PeV. The diffuse neutrino fluxes from GRBs and young pulsars in the range from 100 TeV to 1 PeV are almost the same and lower than the atmospheric background flux. The distribution of estimated diffuse neutrino flux from these young pulsars is narrower than that from AGNs and GRBs; the flux from AGNs and GRBs peaks at about 20 PeV and 1 PeV respectively (He et al. 2012). The neutrino production in young pulsars is constrained by the efficiency of accelerating protons, but the AGNs are more powerful accelerators than pulsars. Perhaps the most violent processes in the universe, such as AGNs or GRBs, could contribute in this energy range. The predicted diffuse neutrinos from pulsars in the Galaxy (Jiang et al. 2007) are easier to detect, because the flux is above the sensitivity threshold of IceCube. The reason why they obtained higher flux than us is because the area of the polar cap that we calculated is different.

The results of diffuse gamma-ray flux are shown in Figure 6. The solid and dashed lines correspond to the fluxes computed for the cases of linear and quadratic proton acceleration respectively.

5 DISCUSSION AND CONCLUSIONS

To summarize, based on the LB model and Bhadra & Dey (2009), we calculate the neutrino and gamma-ray spectrum of some pulsars with an appropriate area for the polar cap. We use the MC method to simulate a pulsar sample with ages less than 10^6 yr and $\boldsymbol{\mu} \cdot \boldsymbol{\Omega} < 0$ in our Galaxy.

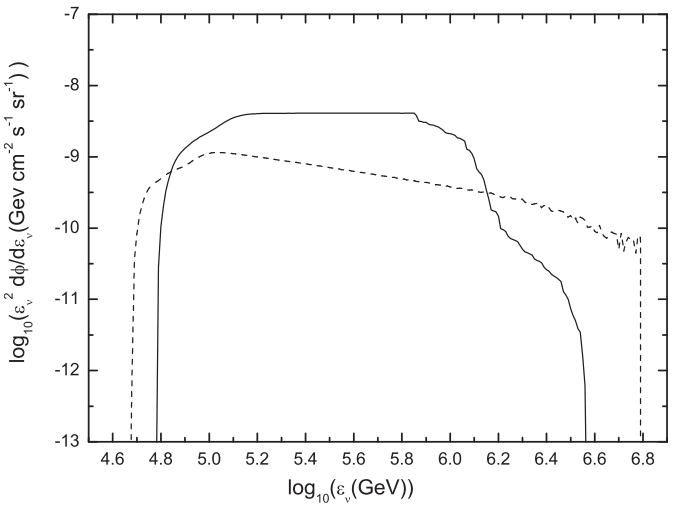

Fig. 6 The estimated diffuse gamma-ray flux from young pulsars in our Galaxy. The solid and dashed lines correspond to the fluxes computed for the cases of linear and quadratic proton acceleration respectively.

By comparing with the ATNF pulsar catalog, our simulation successfully models attributes of the Galactic population of pulsars. Using the sample, we also estimated the flux of diffuse neutrinos and gamma-rays in our Galaxy. Our results show that the diffuse flux, distributed in the energy range from ~ 50 TeV to ~ 3 PeV, is lower by about three orders of magnitude than that of Jiang et al. (2007), only because of the different methods used for dealing with the area of the polar cap.

These results show that the signals of neutrino flux from young pulsars are more difficult to detect, because the energy range, about ~ 50 TeV to ~ 3 PeV, is lower than the sensitivity threshold of IceCube and the atmospheric background neutrino flux. Presently, any statistically significant excess in signals has not been detected from the direction of any pulsar by the AMANDA-II telescope (Ackermann et al. 2005, 2008; Ahrens et al. 2004). These results show that proper consideration of the effect of polar cap geometry in flux calculation is important and pulsars are unlikely to be a strong source of TeV neutrinos. Compared with the flux of diffuse neutrinos with TeV energies emitted from AGNs (Stecker 2005) and GRBs (Liu & Wang 2013), AGNs could be the primary source of TeV neutrinos.

The data on energy of the diffuse gamma-rays from the galactic plane around ~ 50 TeV to ~ 3 PeV have not been found, so we cannot give the percentage of gamma-rays produced through Δ-resonance among all the diffuse gamma-rays in our Galaxy. We expect that experiments like the proposed High Altitude Water Cherenkov (HAWC) detector will continuously survey large regions of the sky, in particular the Galactic plane, at gamma-ray energies up to 100 TeV, with 10 to 15 times the sensitivity of the Milagro detector. If we have the energy data on the diffuse gamma-ray fluxes from the Galactic plane around ~ 50 TeV to ~ 3 PeV, we can estimate the percentage of a pulsar's contribution to this energy range.

This work has some uncertainties, such as the pulsar birth rate and how many pulsars satisfy $\boldsymbol{\mu} \cdot \boldsymbol{\Omega} < 0$. Estimating the flux of thermal photons from the surface of a neutron star is not well determined and the physical processes in the magnetosphere are still not clear, resulting in some uncertainties in the LB model as mentioned by Link & Burgio (2005, 2006). Therefore, in order to improve the prediction of the diffuse muon neutrino and gamma-ray flux from young pulsars, it is crucial to understand more about the neutrino flux and spectra emitted by a single pulsar.

Acknowledgements The authors are indebted to Professor Ze-Jun Jiang for his constructive ideas and helpful suggestions on the manuscript. We thank the referee for helpful comments and suggestions. This work is partially supported by the Science Research Foundation, Department of Education, Yunnan Province (Grant No. 2012Y316) and Yunnan Province under Grant No. 2010CD112.

References

Abbasi, R., Abdou, Y., Abu-Zayyad, T., et al. 2012, ApJ, 745, 45
Ackermann, M., Adams, J., Ahrens, J., et al. 2008, ApJ, 675, 1014
Ackermann, M., Ahrens, J., Bai, X., et al. 2005, Phys. Rev. D, 71, 077102
Aharonian, F., Akhperjanian, A. G., Bazer-Bachi, A. R., et al. 2006, A&A, 457, 899
Aharonian, F. et al. (Hess collaboration). 2007, A&A, 466, 543
Ahrens, J., Bai, X., Barwick, S. W., et al. 2004, Physical Review Letters, 92, 071102
Arons, J., & Scharlemann, E. T. 1979, ApJ, 231, 854
Bednarek, W., Burgio, G. F., & Montaruli, T. 2005, New Astron. Rev., 49, 1
Beskin, V. S., Gurevich, A. V., & Istomin, Y. N. 1993, Physics of the Pulsar Magnetosphere (Cambridge: Cambridge Univ. Press), 117
Bhadra, A., & Dey, R. K. 2009, MNRAS, 395, 1371
Cheng, K. S., Ho, C., & Ruderman, M. 1986, ApJ, 300, 500
Cheng, K. S., & Zhang, L. 1998, ApJ, 498, 327
Daugherty, J. K., & Harding, A. K. 1996, ApJ, 458, 278
Gaisser, T. K., Halzen, F., & Stanev, T. 1995, Phys. Rep., 258, 173
Goldreich, P., & Julian, W. H. 1969, ApJ, 157, 869
Gonthier, P. L., Ouellette, M. S., Berrier, J., O'Brien, S., & Harding, A. K. 2002, ApJ, 565, 482
He, H.-N., Liu, R.-Y., Wang, X.-Y., et al. 2012, ApJ, 752, 29
Hill, G. C., & for the IceCube collaboration 2006, arXiv:astro-ph/0611773
Jiang, Z. J., Chen, S. B., & Zhang, L. 2007, ApJ, 667, 1059
Jiang, Z. J., & Zhang, L. 2006, ApJ, 643, 1130
Kistler, M. D., & Beacom, J. F. 2006, Phys. Rev. D, 74, 063007
Link, B., & Burgio, F. 2005, Physical Review Letters, 94, 181101
Link, B., & Burgio, F. 2006, MNRAS, 371, 375
Liu, R.-Y., & Wang, X.-Y. 2013, ApJ, 766, 73
Manchester, R. N., Hobbs, G. B., Teoh, A. & Hobbs, M. 2005, AJ, 129, 1993
Montaruli, T. 2005, Acta Physica Polonica B, 36, 509
Ribordy, M. 2006, Physics of Atomic Nuclei, 69, 1899
Ruderman, M. A., & Sutherland, P. G. 1975, ApJ, 196, 51
Stecker, F. W. 2005, Phys. Rev. D, 72, 107301
Sturner, S. J., & Dermer, C. D. 1996, ApJ, 461, 872
Zhang, B., & Harding, A. K. 2000, ApJ, 532, 1150
Zhang, L., Cheng, K. S., Jiang, Z. J., & Leung, P. 2004, ApJ, 604, 317